Journal of Molecular Graphics and Modelling 29 (2011) 1030–1038

Contents lists available at ScienceDirect

Journal of Molecular Graphics and Modelling

journal homepage: www.elsevier.com/locate/JMGM

Structural determinants of the alpha2 adrenoceptor subtype selectivity

Liliana Ostopovici-Halip[a,*], Ramona Curpăn[a], Maria Mracec[a], Cristian G. Bologa[b]

[a] Computational Chemistry Department, Institute of Chemistry Timisoara, M. Viteazu 24, 300223, Romania
[b] Department of Biochemistry and Molecular Biology, University of New Mexico School of Medicine, Albuquerque, NM, USA

ARTICLE INFO

Article history:
Received 14 October 2010
Received in revised form 26 April 2011
Accepted 27 April 2011
Available online 6 May 2011

Keywords:
Homology modeling
Docking
GPCR
α2-Adrenergic receptor

ABSTRACT

Alpha2-adrenergic receptor (α2-AR) subtypes, acting mainly on the central nervous and cardiovascular systems, represent important targets for drug design, confirmed by the high number of studies published so far. Presently, only a few α2-AR subtype selective compounds are known. Using homology modeling and ligand docking, the present study analyzes the similarities and differences between binding sites, and between extracellular loops of the three subtypes of α2-ARs. Several α2-AR subtype selective ligands were docked into the active sites of the three α2-AR subtypes, key interactions between ligands and receptors were mapped, and the predicted results were compared with the available experimental data. Binding site analysis reveals a strong identity between important amino acid residues in each receptor, the very few differences being the key toward modulating selectivity of α2-AR ligands. The observed differences between binding site residues provide an excellent starting point for virtual screening of chemical databases, in order to identify potentially selective ligands for α2-ARs.

1. Introduction

The use of computer methods has been successfully applied in numerous studies aiming at the discovery of new potentially active compounds, or at the modification of the existing ones in order to obtain a better biological effect (drug design). The two major types of drug design (ligand-based and structure-based drug design) have different approaches but an identical goal: identification of small active molecules that have complementary shape and charge distribution to the biological target they bind. Structure-based drug design (direct drug design) relies on the three dimensional structure of the biomolecular target obtained through experimental methods such as X-ray crystallography or NMR spectroscopy. Although the number of solved protein structures is continuously growing, there are still a lot of difficulties in obtaining G-protein coupled receptor (GPCR) structures using experimental techniques, since they are membrane-bound proteins. For this reason, molecular modeling studies in general and homology modeling in particular [1] are some of the most widely used techniques for filling the gap between primary sequence and structural information. This approach has been proven extremely relevant especially for the GPCR area [2–5], where the need for three-dimensional information is very stringent due to the lack of high-resolution structural data of their active and inactive states.

The conformational changes that switch between active and inactive states of GPCR have been intensively studied during the last years and many hypotheses have been generated. Recently published crystal structure of a photoactivated intermediate of bovine rhodopsin [6] has shown that the differences between active and inactive states of bovine rhodopsin are minor although previous facts had indicated considerable structural changes [7,8]. On the contrary, the conformational changes triggered due to the GPCR activation by small ligands were not much known. A recent disulfide cross-linking study using the muscarinic M3 receptor revealed new insights regarding the conformational changes associated with receptor activation [9]. Therefore, helices 3, 6, 7 and 8 are involved in receptor activation and the resultant structural changes are somewhat similar, but not identical to those observed in the photoreceptor rhodopsin.

Alpha2-adrenergic receptors (α2-ARs) have a wide distribution in the human body, being responsible for the regulation of many biological and physiological functions such as the control of the central nervous and cardiovascular systems. α2a-AR is the most important subtype from clinical point of view, its stimulation being responsible for the most of the classical effects of α2-AR agonists, like hypotension, sedation, analgesia, lowering of blood pressure, etc. α2b-AR subtype is distributed mainly in peripheral tissues and mediates important physiological responses, such as salt-induced hypertension, vasoconstrictor response to α2-AR agonist gastric mucosal defense, and it has an important role in developmental and reproductive processes [10,11]. The α2c-AR subtype is present in the adrenal medulla, where it mediates the epinephrine release and in the central nervous system (CNS), where it partici-

* Corresponding author. Tel.: +40 724446320; fax: +40 256419824.
E-mail address: lili.ostopovici@acad-icht.tm.edu.ro (L. Ostopovici-Halip).

1093-3263/$ – see front matter © 2011 Elsevier Inc. All rights reserved.
doi:10.1016/j.jmgm.2011.04.011

pates with α2a-AR in the presynaptic inhibition of norepinephrine release [12].

α2-ARs are attractive targets for the treatment of several general diseases like hypertension, pain, depression, anxiety, and obesity, thus their specific agonists and antagonists would have important therapeutic applications. However, because of the common mechanisms for the signal transduction and the very high degree of sequence homology (more than 80%) exhibited by α2-ARs, information regarding subtype-selective compounds is still limited. At the time of this manuscript preparation, only a few compounds have been reported to be α2-ARs subtype-selective: the agonists guanfacine for α2a-AR and R-(+)-m-nitrobiphenylinde oxalate for α2c-AR and the antagonists BRL-44408 for α2a-AR, JP-1302 and OPC28326 for α2c-AR [13–19].

As a follow-up of our previous works [20,21], this paper combines structural bioinformatics approaches like homology modeling and docking to identify the main molecular characteristics which regulate the selectivity within the α2-ARs subtypes. For this purpose we have built the three dimensional structure of each α2 receptor subtype and analyzed their binding sites to find structural differences that could guide the design of new selective ligands.

2. Results and discussion

2.1. Homology models of α2-ARs

For many years the bovine rhodopsin has been the only GPCR with experimental structural information available, and all the homology modeling efforts were focused on this structure [22,23]. During the last few years, other GPCR protein structures have been solved: the human β2 adrenergic receptor [24], the turkey β1 adrenergic receptor [25], the squid rhodopsin [26] and the human adenosine A2a receptor [27]. Although the squid rhodopsin has the highest sequence similarity with α2-ARs, the β2 adrenergic receptor (β2-AR) structure (PDB code: 2rh1) was chosen as structural template because it belongs to the GPCR-class A subfamily and binds a biogenic amine like α2-ARs. These criteria proved to be successful in other cases, too [28].

The alignment of the amino acid sequences generated by the T-coffee server [29,30] was manually refined using as a guide the three dimensional structure of the β2-AR to avoid the placement of the insertions or deletions in the transmembrane domains. For each loop, the deletions or insertions were grouped into one single section which was placed in the most adequate point consistent with the template structure. The disulfide bridge between the second extracellular loop (EL2) and the extracellular part of the third transmembrane helix, conserved in most GPCRs, was taken in consideration during the model building process (double underlined in Fig. 1). In all three α2-ARs, the C-terminal part and the third intracellular loop (IL3), which are over 100 residues long, were not modeled because the available loop modeling algorithms are limited to up to 13 residues long loops.

The homology models for α2-ARs have been generated based on the alignment in Fig. 1 and using the crystal structure of beta2-AR as template. The resulted models have been energy minimized using the OPLS2005 force field [31] implemented in the Protein Preparation Wizard module [32] of the Schrodinger package.

For an easier understanding, in the present paper the homology models of α2-ARs will be further mentioned as Ma (α2a-AR), Mb (α2b-AR) and Mc (α2c-AR). For the same reason, specific amino acids from the transmembrane helices were named using the numbering system proposed by Ballesteros and Weinstein in 1995 [33]. Briefly, for the most highly conserved residue in each transmembrane helix is assigned a value of 50, preceded by the number of the transmembrane helix: Asn1.50, Asp2.50, Arg3.50, Trp4.50, Pro5.50, Pro6.50, and Pro7.50 (see Fig. 1). The other residues on the same helix will have a value corresponding to their position relative to the most conserved residue in transmembrane. The amino acids belonging to the intra or extracellular loops are identified by the corresponding number in the sequence (Val36, Asp135, etc.).

Previous mutagenesis studies on α2a-AR [34] have shown that substitution of Asp3.32 with an asparagine produces EC50 values 500-fold higher than those for the wild-type, suggesting an involvement of this amino acid in the ligand binding. Also, the biological characterization of the Ser5.46Ala mutant has revealed a possible role of Ser5.46 residue in hydrogen bond formation with the *para*-hydroxyl group on the phenyl ring of catecholamines. To check if Ma, Mb and Mc models confirm and support this essential information, we performed a docking test using noradrenaline (norepinephrine), the endogenous ligand of all adrenergic receptors. Using SiteMap [35], the primary binding site of Ma model was located in the extracellular part of the transmembrane domain, within a cavity defined by residues from helices 3, 5, 6 and 7. This position was identified as the active site in other GPCRs structures [22–28,34,36]. For an accurate prediction of the norepinephrine geometry in the binding site we used Schrodinger's Induced Fit Docking (IFD) method which merges the predictive power of Prime with the docking and scoring capabilities of Glide [37,38]. The results from IFD have shown a ligand conformation for the α2a-AR which is in agreement with the mutagenesis data. The best pose of norepinephrine is located in the transmembrane domain in a crevice positioned in the extracellular half of the protein exactly where the GPCR binding pocket is located [22–28,34]. The ligand is oriented parallel with the membrane and the amino and hydroxyl groups point toward helices 3 and 5, respectively. The positively charged nitrogen atom is placed at about 3.13 Å from Asp3.32 side-chain, and is favorably oriented to establish an electrostatic interaction with its negatively charged COOH functional group. The benzene ring is surrounded by a hydrophobic environment defined by several aromatic amino acids placed on helices 5 and 6: Tyr5.38, Phe6.52 and Phe6.53. The hydroxyl group in the *para* position interacts through a hydrogen bond with the hydroxyl group from Ser5.46 side-chain (depicted in red in Fig. 2). (For interpretation of the references to color in this figure, the reader is referred to the web version of the article.)

Similar conformations of norepinephrine were found for the other two α2-ARs (Mb and Mc models). The carboxyl group from the Asp3.32 side-chain forms a salt-bridge with the quaternary amino group of norepinephrine (3.13 Å in Mb and 3.34 Å in Mc), while Ser5.46 forms hydrogen bonds with the catecholic hydroxyl group.

All this information is in agreement with experimental data obtained through site-directed mutagenesis and supports the further use of the homology models in our study.

2.2. Binding site analysis

The position of the binding sites indicated by SiteMap is in agreement with what is known about GPCR binding from literature and mutagenesis data [34,36]. Because of the high sequence similarity of α2-ARs, the predicted hydrophilic and hydrophobic surfaces are comparable between the three proteins, the major difference being the size of their binding sites (598.6 $Å^3$ in α2b-AR, 683.3 $Å^3$ in α2b-AR and 513.6 $Å^3$ in α2c-AR).

During the inspection of the three α2-ARs binding sites, a very high sequence identity was noticed for the amino acids found in the immediate vicinity of the docked norepinephrine. We found that apart from nine amino acid variations (Table 1), all the residues placed at less than 6 Å around norepinephrine are identical, which suggests a reasonable explanation for the scarcity of selective ligands for this receptor family. Three of the nine amino acid variations

Fig. 1. Sequence alignment between human β2-AR and α2-ARs. The transmembrane domains in the template structure are shown in italics and the highly conserved residues in gray. The sulfur bridge between the two cysteine residues from helix 3 and EL2 is double underlined. Positions x.50 are enclosed into black boxes.

Table 1
Sets of different amino acids occupying the same position around the endogenous ligand (6 Å).

α2a-AR	α2b-AR	α2c-AR	Location	Position on TM	Amino acid variation
V86	I65	V104	TM2	2.57	AAV1
K174	D153	R192	EL2		AAV2
I190	L166	L204	EL2		AAV3
D192	Q168	D206	EL2		AAV4
V197	I173	I211	TM5	5.39	AAV5
C201	S177	C215	TM5	5.43	AAV6
T397	G394	Y405	TM6	6.58	AAV7
R405	H405	G416	TM7	7.32	AAV8
K409	Q409	K420	TM7	7.36	AAV9

(AAV) are located on the second extracellular loop (EL2) between helices 4 and 5, whereas the other six are on the transmembrane helices. Obviously, not all the residues from this selected group of amino acids that are found in the close vicinity of the docked norepinephrine contribute equally to the ligand binding, but key residues involved in binding are expected to be found in this set. A special attention has been dedicated to these nine variations (see Fig. S1 of Supplementary data) which together with the size of the binding site are the only differences we have noticed in that region.

For the first variation we have examined, the presence of a valine residue in α2a-AR and α2c-AR and an isoleucine residue in α2b-AR at the position 2.57 (Val86/Ile65/Val104, AAV1), does not make a big difference in the properties of the binding site. Valine and isoleucine display similar topological and physicochemical characteristics like a C-beta branch, non-reactive side chains, and similar hydrophobicity, but also some differences like volumes, sizes and surfaces. Although a valine residue allows for the ligand to accommodate a larger substituent than an isoleucine residue does, it is expected that a ligand which can easily discriminate between these two residues would be difficult to find. An identical circumstance was observed at position 5.39 occupied by a valine residue in α2a-AR and an isoleucine residue in α2b-AR and α2c-AR (Val197/Ile173/Ile211, AAV5). Similarly, the presence at the same position on EL2 of an isoleucine residue in α2a-AR and a leucine residue in α2b-AR and α2c-AR (Ile190/Leu166/Leu204, AAV3) does not dramatically affect the properties of the binding site, because in both situations the pocket contains an aliphatic, hydrophobic residue with identical size (the same molecular weight), volume, and a comparable surface. However, a first significant difference in the α2-ARs binding sites was noticed at position 5.43, filled by a Cys residue in α2a-AR and α2c-AR and a Ser residue in α2b-AR (AAV6). Compared to cysteine, serine is small, less hydrophobic and slightly polar, even if it is rather neutral. Cysteine has a bulky side-chain, very hydrophobic, which can also function as a nucleophilic group.

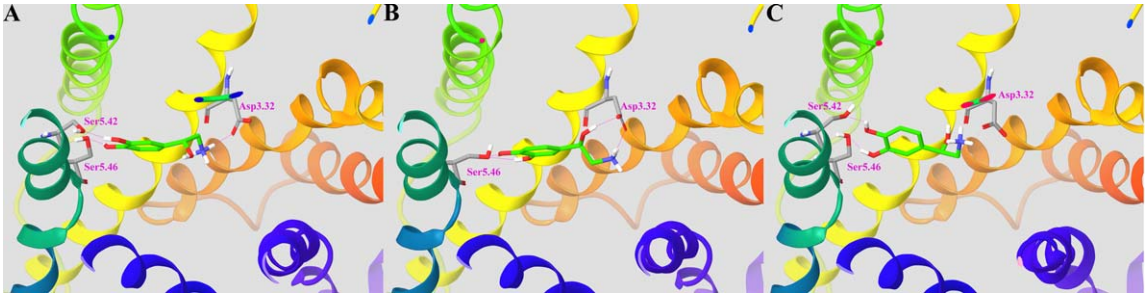

Fig. 2. Docked nor-epinephrine in the α2a-AR (A), α2b-AR (B) and α2c-AR (C).

The hydroxyl group in the serine side-chain could be involved in the formation of hydrogen bonds with the protein backbone or with diverse polar functional groups from ligands. Due to its location and vicinity in α2a-AR and α2c-AR, Cys5.43 cannot be involved in disulfide bond formation with other cysteine residues. This "mutation" can be explored in the design of new α2-ARs subtype selective compounds by selecting the right substituent for each type of receptor: a polar substituent for α2b-AR which interacts with Ser5.43 side-chain through a hydrogen bond or a sulfur-containing substituent or a related bioisoster for α2a-AR and α2c-AR. Also, the contribution of this residue to the agonist binding mode at adrenergic receptors has been recently reported [39].

The pair aspartate–glutamine on EL2 (AAV4) also suggests a possible direction in the process of designing new selective compounds for α2b-AR. Aspartic acid and glutamine are polar amino acids, but the size and the net charge of their side-chains are different. Asp192 and Asp206 in α2a-AR and α2c-AR subtypes contain a side-chain carboxyl group which is negatively charged unlike Gln168 in α2b-AR that is a polar but uncharged amino acid. A positively charged substituent might be the perfect pair to create a stabilizing salt-bridge with the ligand in the case of α2a-AR and α2c-AR, and a hydroxyl or ether substituent might be a suitable partner for a hydrogen bond formation in α2b-AR. A similar association of amino acids is noticed at the beginning of helix 7, in the 7.36 position: Lys7.36 in α2a-AR and α2c-AR and Gln7.36 in α2b-AR (AAV9). Compared with lysine, glutamine is a smaller, uncharged, and slightly polar amino acid, and may be involved in hydrogen bond interactions with functional groups from ligands. Lysine is a positively charged amino acid which is prone to form salt-bridge interactions.

We believe that all these differences revealed through binding site analysis represent an excellent starting point for further studies aiming at discovery of selective α2-ARs ligands. One might argue that all these differences might occur because of an inaccurate alignment and/or modeling of the loops or transmembrane helices. But an incorrect alignment of the transmembrane domains is very unlikely to happen because we did not allow insertions or deletions within the transmembrane domain and the highly conserved residues of each transmembrane helix were aligned according to Baldwin's model for the alpha-carbon positions in the seven transmembrane helices of the GPCR family [40]. Six out of the nine mentioned variations are located in the transmembrane region, only three being situated on the second extracellular loop. Except for the cysteine residue from EL2, there is no other known conserved residue on this extracellular loop across the GPCR family. Thus, we have decided to check if the location of AAV2, AAV3 and AAV4 variations on EL2 is a real fact or it is the consequence of a wrong alignment. For this purpose, the entire EL2 of each α2-AR model (Glu173-Gln193 in Ma, Gly152-Glu169 in Mb and Tyr191-Glu207 in Mc) was rebuilt *de novo* without any alignment with template structure. The new obtained models will be further mentioned as M1a, M1b and M1c, respectively (depicted in gray in Fig. 3). Given that the spatial arrangement of the EL2-s differs significantly in M1 receptors as a consequence of different lengths of EL2 in each subtype, no similarity between the positions of these three variations was noticed (Fig. 3).

In the β2-AR crystal structure and also in Ma, Mb and Mc models, EL2 is folded above the binding cavity, covering the top of the active site like a lid. In each M1 model obtained by *de novo* modeling of EL2 from the M models, EL2 is placed outside of the transmembrane domain and the top of the binding site is wide-open. In these circumstances, it is not important if the previously mentioned amino acid differences are really aligned or not, because they would have little or no influence on the ligand binding mode.

Furthermore, in all of the M1 models (gray in Fig. 3) the conserved cysteine in EL2 is unable to form the disulfide bridge with the cysteine residue located on the extracellular side of the helix 3. This disulfide bridge is highly conserved in the GPCR family, being considered critical for stabilization of the ligand in the binding site and/or proper receptor folding. To preserve this characteristic, another *de novo* modeling of EL2 was performed and this time a constraint was added – disulfide bridge formation. For this purpose, the sulfur–sulfur bond was used as an anchor point by keeping rigid the coordinates of Cys188 (α2a-AR), Cys164 (α2b-AR) and Cys202 (α2c-AR), similarly with the initial Ma, Mb and Mc models (black in Fig. 3). The two resulted fragments for EL2 were modeled concurrently. Fragment 1 contains the residues located between the last amino acid on helix 4 and the cysteine residue on EL2 (Cys188 in Ma, Cys164 in Mb and Cys202 in Mc), and it also includes the AAV2 variation (Lys174/Asp153/Arg192). Fragment 2 contains the amino acids positioned after the disulfide bridge up to the first residue on helix 5 and includes the other two differences enclosed in EL2: Ile190/Leu166/Leu204 (AAV3) and Asp192/Gln168/Asp206 (AAV4). The resulted models will be further called M2a, M2b and M2c receptors.

In each M2 model, the second half of EL2 (fragment 2) was predicted *de novo* in a similar manner with Ma, Mb and Mc models (see Table S1 of Supplementary data). On the contrary, when fragment 1 was built without any alignment between α2-ARs and β2-AR sequences (gray in Fig. 4), the spatial arrangements of fragment 1 are pretty different than those resulted via homology modeling (black in Fig. 4). This remarkable discrepancy can be explained by EL2 similarity between α2-ARs and β2-AR: fragment 1 exhibits no sequence similarity while fragment 2 shows around 30% similarity.

Most likely, the AAV3 and AAV4 variations enclosed in fragment 2 are preserved very well also in M2 models (Fig. 4). The involved amino acids, Ile190/Leu166/Leu204 (AAV3) and Asp192/Gln168/Asp206 (AAV4), occupy analogous positions on EL2 and have the same orientation of the side-chains, toward the interior of the transmembrane helical bundle.

However, the critical variation AAV2 enclosed in fragment 1 presents a different alignment of the involved amino acids. The positively charged residues Lys174 in α2a-AR and Arg192 in α2c-AR have similar positions and side-chain orientations in M2 models, but we cannot say the same thing about Asp153 from α2b-AR. This residue is found at a different position when compared with its initial position from M2b models, due to a wider curvature at the beginning of EL2, caused by the presence of Gly152. Probably, this arrangement is more realistic than the initial model obtained using homology, because in the *de novo* modeling the conformational flexibility of glycine is taken in consideration. For the same reason, we have chosen to use these models (M2) in further docking experiments.

2.3. Virtual screening experiment

To test the ability of M2a, M2b and M2c models to discriminate between active and inactive compounds, a virtual screening experiment was carried out using a library which contains α2-ARs active compounds seeded between a set of randomly selected decoys. The actives represent approximately 8% of the entire set of compounds and they were selected based on the biological activity expressed against alpha2 subtypes.

The docking simulations were performed on each model using a library of 1730 compounds seeded with 129 actives selected from the Wombat database [41,42] and 1601 compounds selected from the Database of Useful Decoys (DUD) [43,44]. The experimental values of biological activities range from high micromolar to high nanomolar. The decoys selection process was conducted in part randomly and in part directed toward the drug-like molecules using cutoffs for molecular weight, log *P* and number of rotatable bonds. Also, it has to be emphasized that we have tried to select the set

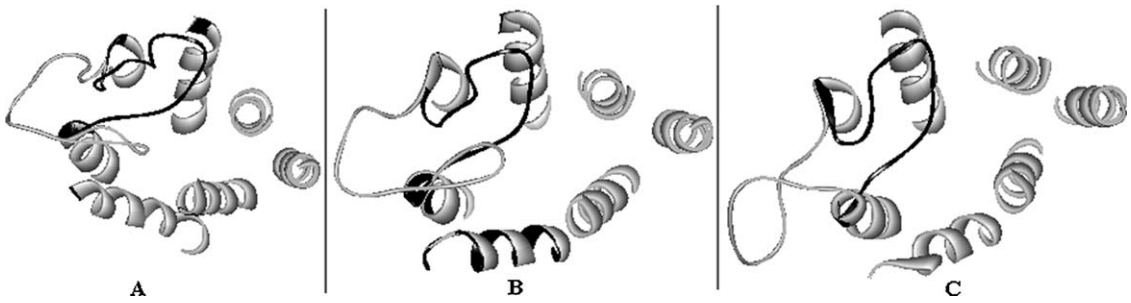

Fig. 3. Superposition of the homology models of the α2-ARs built based on the alignment in Fig. 1 (black) and the new models with EL2 modeled *de novo* (gray). For clarity only extracellular part of the transmembranes is shown and the other loops were hidden. A-α2a-AR, B-α2b-AR, C-α2c-AR.

of decoys having a molecular weight distribution similar to that of the actives set.

The models ability to recover the actives from the library was assessed by enrichment validation. The enrichment factor quantifies the number of active compounds from a selected subset of the ranking list relative to the entire database. In this study the enrichment factors (EF) were calculated using the following equation:

$$EF = \frac{Hits_{selected}}{Hits_{total}} \times \frac{N_{total}}{N_{selected}}$$

where $Hits_{selected}$ represents the number of actives found at a specific threshold level (percentage) of the database screened, $Hits_{total}$ represents the total number of actives in database, N_{total} represents the total number of compounds in the entire database and $N_{selected}$ represents the number of compounds in the selected subset of the ranked database.

Because in the current study a dataset enriched by approximately 8% (129 actives and 1601 inactives) was screened, the best reachable performance for each model will be 100% (129 of 129) at top 8%, corresponding to an EF = 13.4. At this threshold the maximum enrichment factor has not been achieved for any of the models. Therefore, enrichment factors were calculated at top 2%, 5% and 10% of the scored and ranked dataset.

As can be seen from Table 2, the virtual screening experiments performed on the three models produced a significant prioritization of ligands versus decoys. When top 2% of the library was considered the maximum enrichment factor for each model was obtained (Table 2).

Table 2
Enrichment factors calculated for each model at different levels of sampling of the dataset.

Model	Enrichment factors (EF)		
	2%	5%	10%
M2a	13.0	13.0	8.3
M2b	13.0	11.86	6.12
M2c	13.0	12.02	6.05

For the M2a model a similar performance was observed at the 5% threshold level, but the enrichment factor has decreased to 8.3 at 10% threshold. The M2b and M2c models perform almost similarly in retrieving actives at 5% and 10% levels, with comparable EF values, but poorer when compared to M2a.

The virtual screening experiments conducted for the α2-AR homology models have shown that these models perform well, identifying known actives hidden in a database of decoys. This exercise proved that the models are robust and can be reliably used in further experiments.

2.4. Docking

A docking experiment was set up to check if AAV1–AAV9 variations are involved in the binding mode of several α2-AR subtype-selective antagonists (Fig. 5) and to see if these models could address the issue of subtype selectivity. The ligands were docked into each model and the analysis of the docking poses list for each α2-AR subtype was performed, according to their

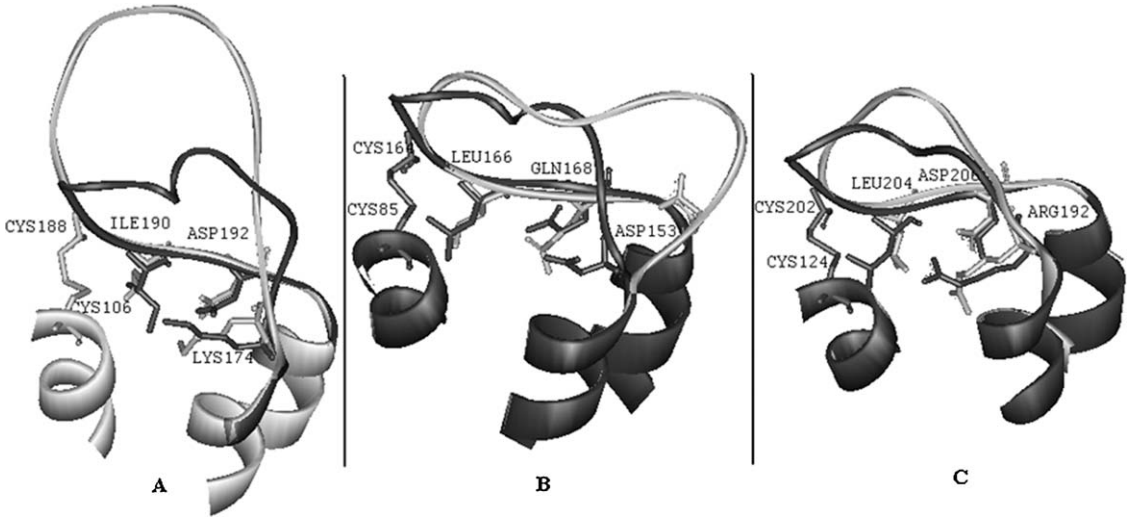

Fig. 4. Superposition of the homology models of the α2-ARs built based on the alignment in Fig. 1 (black) and the homology models with EL2 modeled *de novo* (gray). For clarity only the extracellular part of helices 4 and 5 are shown. A-α2a-AR, B-α2b-AR, C-α2c-AR.

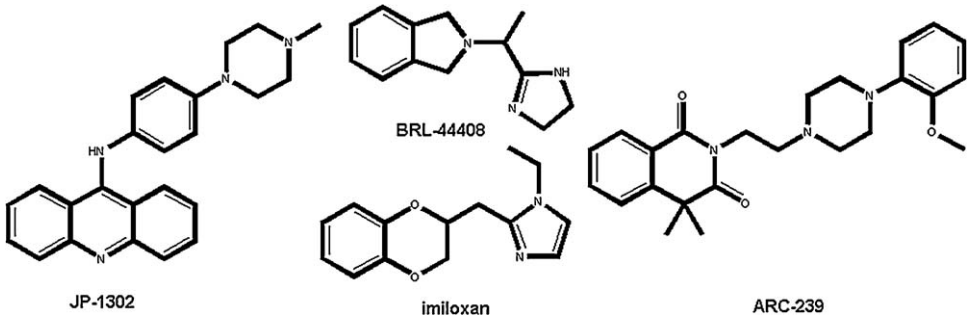

Fig. 5. Chemical structures of α2-AR-selective antagonists used in the docking tests.

docking scores. Ideally, in a docking experiment the compounds should be sorted according to their biological activity, which should be reflected by the docking scores. From the docking results, we noticed that the selective ligands of each subtype (having the highest biological activity for that particular subtype) were ranked at the top of the docking poses list for each of the three models. For example, BRL-44008, a selective α2a-AR antagonist, was ranked first on the docking poses list obtained for the model of the α2a-AR subtype relative to the other compounds, fourth for α2b-AR and third for α2c-AR, respectively (see Table S2 of Supplementary data). Thus, the selectivity profile of each docked antagonists was roughly reproduced by the models. Although these results suggest the models' ability to discriminate between selective ligands, we believe that it is too soon to generalize the observed information obtained through docking experiments, because the number of known selective antagonist is too small. Nonetheless, we strongly believe this information would be definitively useful for the discovery and designing of new selective alpha2 antagonists.

A direct interaction of the AAV2 and AAV7 variations with ligands has not been anticipated, mainly because of their positions compared to the active site. AAV2 is positioned on the EL2 very close to the extracellular end of helix 4 and it is somehow distant from the active site due to the orientation of helix 3 in the GPCR family [45]. Also AAV7 is located at the junction between helix 6 and EL3, high above the binding cavity. Surprisingly, these two variations do interfere with some ligands, as it will be shown next.

Induced fit docking of BRL-44408 has revealed that AAV2, AAV3 and AAV4 variations work together to differentiate the binding mode of this compound that acts as an α2a-AR selective antagonist [46,47]. Thus, in the α2a-AR binding site (Fig. 6a), the imidazoline ring of BRL-44408 is positioned between helices 3 and 6 and the rest of the molecule, containing an isoindole moiety, is placed in a hydrophobic pocket defined by Phe6.52, Phe6.53 and Val3.33 residues. Furthermore, the protonated nitrogen atoms of the imidazoline ring interact with the receptor as follows: one atom is hydrogen bonded to the Tyr6.55 residue, whereas the other one is engaged in an electrostatic interaction with Asp3.32 side-chain (Fig. 6a). The presence of a leucine residue on EL2 in α2b-AR instead of an isoleucine in the α2a-AR subtype (AAV3) pushes the imidazoline ring away from helix 6 and the hydrogen bond with Tyr6.55 cannot be established. Still, a new hydrogen bond is formed with Gln168 corresponding to AAV4 (Fig. 6b). The α2c-AR subtype also contains a leucine residue at the AAV3 position, but BRL-44408 adopts a totally different orientation in the α2c-AR binding site compared to the other two AR subtypes. Accordingly, the best pose of BRL-44408 in the α2c-AR binding site is aligned parallel to the membrane and not perpendicular to it as in the case of α2a-AR and α2b-AR subtypes (Fig. 6c). This particular arrangement is caused by the swing of Asp206 side-chain (AAV4) toward Arg192 (AAV2) to whom it forms a salt bridge, leaving more space in the α2c-AR binding site. Even if position AAV4 from α2a-AR subtype is also occupied by an aspartic acid, position AAV2 is not filled with an arginine residue, and the salt bridge contact cannot be established. Moreover, the aspartic acid side-chain points toward the interior of the transmembrane domain, and a parallel orientation of the ligand to the membrane is not possible. Besides all these aspects, BRL-44408 has the best complementary orientation against the α2a-AR binding site (see Fig. S2 of Supplementary data).

The molecular docking experiments of JP-1302, a selective antagonist of the α2c-AR subtype [18,19], have yielded different binding modes for each α2-ARs binding sites (Fig. 7), mostly due to the AAV8 variation. The AAV7 and AAV9 variations also play an important role. The glycine residue found at position AAV8 in the α2c-AR subtype allows for the accommodation of the ligand's acridine ring into a hydrophobic pocket located in the extracellular part of the receptor, between the upper parts of helices 6 and 7. This position is occupied by larger residues, histidine in the case of alpha2a-AR and arginine in the case of alpha2b-AR, which obstruct the acridine ring, and implicitly the entire ligand, to adopt a similar orientation as in the α2c-AR binding site. The

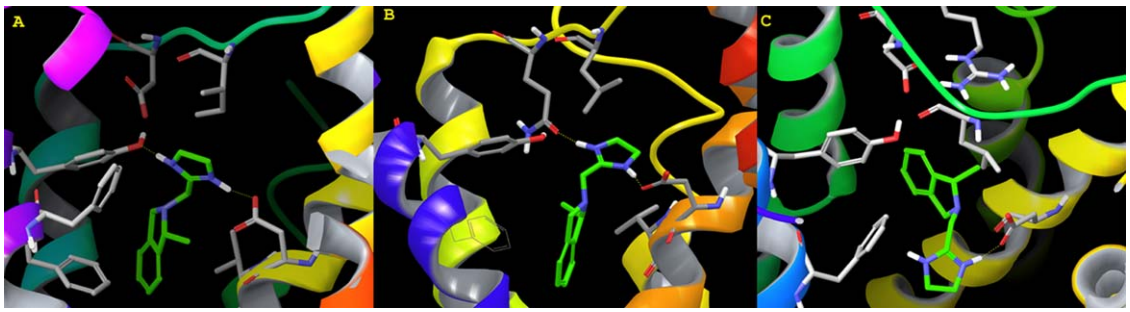

Fig. 6. BRL-44408 (green) into the α2a -AR (A), α2b-AR (B) and α2c-AR (C) binding sites.

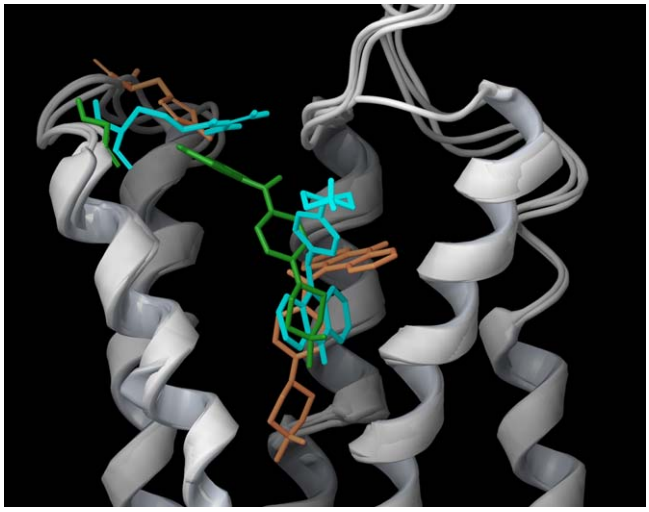

Fig. 7. JP-1302 into the α2a-AR (blue), α2b-AR (orange) and α2c-AR (green) binding sites. (For interpretation of the references to color in this figure legend, the reader is referred to the web version of the article.)

JP-1302 binding mode at the α2c-AR binding site is characterized by the formation of a salt bridge between Asp3.32 and the protonated nitrogen atom of the piperidine ring and a hydrogen bond between Tyr6.58 (AAV7) and the nitrogen atom of the acridine ring. Additionally, the hydrophobic parts of the ligand are favorably oriented in the hydrophobic cavities of the binding sites. For example the acridine ring is surrounded by aromatic residues like Phe7.35, Tyr6.55, Tyr6.58 and the hydrophobic part of Lys7.36 side-chain (AAV9). The phenyl linker is lined by the Phe7.39 and Phe6.51 residues, and the methyl substituent of the piperidine ring is flanked by the Trp6.48 and Cys3.37 residues (see Fig. S3 of Supplementary data).

Imiloxan has been reported as an α2b-AR subtype-selective compound [48] but it has been tested only against the rat α2a-AR and α2b-AR subtypes, thus its selectivity refers mainly to α1-ARs subtypes. pK_i values against the human α2-ARs show imiloxan as a potent antagonist of α2b-AR, but its selectivity is not convincing [49]. Other compounds with a pharmacological profile similar to imiloxan have been recently reported [50,51] but again they have not been evaluated against all three α2 subtypes. ARC-239 shows a similar biological profile with imiloxan and it exhibits good activity against the α2b-AR and α2c-AR subtypes and weak activity on the α2a-AR subtype [47]. The molecular docking has revealed that AAV2 and AAV4 variations are determinant factors for the ARC-239 binding to the α2-ARs subtypes, the most significant differences consisting in the spatial arrangement of the best poses. In the α2b-AR subtype, the ligand fits the cleft between the second extracellular loop and helices 3–5 being perpendicular on the membrane. The anisole moiety is positioned right under EL2 and it points toward the upper parts of the helices 3 and 4. In addition to the hydrogen bonds between the isoquinoline-1,3-diketone ring and Tyr5.38 and Tyr6.55, a hydrogen bond is formed between one of the two nitrogen atoms of the piperidine ring and Gln168 (AAV4). In the α2a-AR and α2c-AR binding sites, ARC-239 adopts an orientation parallel to the membrane and the factors responsible for these spatial arrangement differences are the AAV2 and AAV4 variations. In α2a-AR and α2c-AR these positions are occupied by an aspartic acid residue (AAV2) and a lysine or arginine residue (AAV4). The side chains of Asp192 and Lys174 in α2a-AR and Asp206 and Arg192 in α2c-AR, respectively, are pointing to each other due to their charges and they are filling the cavity where the anisole ring lays when ARC-239 is binding to α2b-AR.

3. Methods

3.1. Sequence alignment

The sequences of the human α2a-AR, α2b-AR and α2c-AR were extracted from the SWISS-Prot database [52,53] (accession codes: P108913, P18089 and P18825) in Fasta format and were automatically aligned using the T-coffee server [29,30] with the sequence of the human β2-adrenergic receptor taken from the RSCB Protein Data Bank (accession code: 2RH1). The lyzozome T4 fragment was removed from the sequence of the β2-AR crystal structure, and the final alignment was further manually refined.

3.2. Model building and loop modeling

The homology modeling package Modeller [54,55] (version 9v6) was used to generate the three-dimensional models for α2-ARs based on the X-ray structure of β2-AR using the sequence alignment presented in Fig. 1. The resulting models were first geometrically refined in order to reduce the side chains steric clashes. Subsequently the entire receptor, including the main backbone, was energetically minimized. The final models have over 90% of residues in the favorable regions of the Ramachandran map and all the main-chain parameters, like peptide bond planarity, bad non-bonded interactions, Cα distortion, overall G-factor, bond length distribution and side-chain parameters, are in the normal range. When necessary, the second extracellular loop (EL2) of the α2-AR subtypes was built without any alignment with β2-AR, using the Modeller's routine MODLOOP, explicitly designed for loop modeling [56,57]. In these cases the final models were also energy minimized.

3.3. Binding site identification

The location of the primary binding site in the α2-ARs was determined using results from mutagenesis studies and computational prediction with the SiteMap 2.1 application from the Schrödinger software package [35]. In the first step of the SiteMap procedure, a grid is set up and one or more regions on the protein surface that are suitable for ligand binding are identified. Next, contour maps are drawn generating hydrophobic and hydrophilic regions, and in the final step various properties are evaluated for each site.

3.4. Ligand docking

Ligand setup. LigPrep 2.1 [58] was used to prepare the ligands for docking. The hydrogen atoms were added to the ligand compounds and the possible tautomers at physiological conditions were generated. Finally, the ionization states were set and the final geometries were minimized using the OPLS2005 force field [31].

Protein setup. Protein Preparation Workflow [32] was used to add all the hydrogen atoms to the homology models of α2-ARs, and to optimize the charge states of Asp, Glu, Arg, Lys, and His residues and the orientation of hydroxyl and amide groups. Finally, a restrained minimization was performed using the Impref utility, which is based on the Impact molecular mechanics engine [59] and the OPLS2005 force field, using a max RMSD of 0.20.

Docking protocol. The binding properties of the endogenous ligand and subtype-selective compounds were explored with the Induced Fit protocol based on Glide 4.5 [37] and Prime 1.6 [38]. The procedure starts with a preliminary docking of the ligands in the receptor binding site, when 20 poses per ligand are retained, followed by the refinement of the side chains of residues found within 8 Å of an atom in any of the 20 poses. The complexes within 30 kcal/mol of the minimum energy structure are further used in the final docking step when ligands are redocked into each

of the refined receptor structures. The final poses are ranked by a combined score composed of the Glide score (receptor–ligand interaction energy) and the Prime energy (receptor strain and solvation energy).

In a preliminary run, the endogenous ligand was docked in a grid-box chosen to include the entire protein. In the following runs, the docking grid was centered on the 3.33 position of each of the α2-AR subtypes and the size of the box was set at 30 Å on each side.

3.5. Virtual screening experiment

Ligands set preparation. The set of ligands active against α2-ARs was compiled from the Wombat 2007.1 database [41,42] which is a collection of chemical and biological information carefully curated from the medicinal chemistry literature. The compounds were selected to satisfy the following criteria:

- tested against at least one of the α2-AR subtypes;
- biological activity expressed as pIC_{50}, pK_i greater than 8.

A set of decoys was prepared by selecting compounds from the database of useful decoys (DUD) [43,44]. Briefly, the decoy sets for all 40 targets were gathered and a superset containing 124,431 molecules was obtained. After the removal of duplicates, tautomers and structures that we could not be processed, a set of 91,311 ligands was compiled with the help of InstantJchem [60]. The compounds were further filtered by applying the following drug-like criteria in the selection process:

- molecular weight between 200 and 600 Da;
- number of rotatable bonds between 1 and 10 Da;
- at least one polar atom (N, O, S);
- log *P* value between −6 and +6.

Finally, a set of 1601 compounds was compiled. By combining these compounds with the set of 129 active ligands, a final set of 1730 compounds was gathered and processed with the ligand preparation utility LigPrep [58], as previously described. Thus, a set of actives and decoys ready for docking studies was obtained.

Protein preparation. The 3D-models of the receptors were prepared with Protein Preparation Workflow as previously described.

Docking setup. Glide receptor grids were generated from the prepared receptor models, with the docking grids centered on position 3.33 of each α2-AR subtype: Val114 (α2a), Val93(α2b), and Val132 (α2c). The binding site was defined by a docking box with dimensions of 20, 14, and 14 Å. The docking runs were performed with Glide 4.5 [37] in SP mode using the default settings for parameters. No scaling factors were applied to the van der Waals radii of the receptor atoms, and the default value of the scaling factor of 0.8 was applied to the non-polar atoms of the ligands database. The free rotation of the hydroxyl groups of the residues from the binding cavity was allowed.

4. Conclusions

Molecular and homology modeling of the α2-ARs subtypes still represents a very motivating topic as confirmed by the high number of studies published so far. The present study shows the successful application of homology modeling to the building of three dimensional models for α2-ARs subtypes based on the X-ray structure of the β2-adrenergic receptor. The models have reproduced the experimental data regarding the binding of the endogenous ligand and also performed very well in a virtual screening experiment using a library of 1730 compounds. These results provide evidence that the *in silico* models developed in this work are reliable and robust, being powerful tools which can be used in further virtual screenings. Docking runs performed with different selective ligands against the α2-ARs subtypes allowed us to perform a detailed analysis of the common and more important, the specific elements of these receptors' binding cavities. The analysis revealed a strong identity between the important amino acids in each receptor binding site. Still, a few differences have been noticed, and these differences are the key elements which can be exploited in virtual screening of chemical databases for discovery of selective α2-AR ligands. Our results suggest that the residue differences in the binding site presented in this study should be taken into consideration and be given a certain weight in the process of searching for α2-AR subtype-selective compounds.

Acknowledgements

This work was supported by the National Council for Scientific Research in Higher Education (CNCSIS) grant PN-II-PCE-ID nr 1268/Agreement 248/2007 and additional agreement 2/2009, and by the NIH 1U54MH084690 and NCRR P20 RR016480 grants to CGB.

Appendix A. Supplementary data

Supplementary data associated with this article can be found, in the online version, at doi:10.1016/j.jmgm.2011.04.011.

References

[1] C.N. Cavasotto, S.S. Phatak, Homology modeling in drug discovery: current trends and applications, Drug Discov. Today 14 (2009) 676–683.
[2] F.M. McRobb, B. Capuano, I.T. Crosby, D.K. Chalmers, E. Yuriev, Homology modeling and docking evaluation of aminergic G protein-coupled receptors, J. Chem. Inf. Mod. 50 (2010) 626–637.
[3] O.M. Becker, S. Shacham, Y. Marantz, S. Noiman, Modeling the 3D structure of GPCRs: advances and application to drug discovery, Curr. Opin. Drug Discov. Devel. 6 (2003) 353–361.
[4] A. Patny, P.V. Desai, M.A. Avery, Homology modeling of G-protein-coupled receptors and implications in drug design, Curr. Med. Chem. 13 (2006) 1667–1691.
[5] F. Fanelli, P.G. De Benedetti, Computational modeling approaches to structure–function analysis of G protein-coupled receptors, Chem. Rev. 105 (2005) 3297–3351.
[6] D. Salom, D.T. Lodowski, R.E. Stenkamp, I. Le Trong, M. Golczak, B. Jastrzebska, T. Harris, J.A. Ballesteros, K. Palczewski, Crystal structure of a photoactivated deprotonated intermediate of rhodopsin, Proc. Natl. Acad. Sci. U.S.A. 103 (2006) 16123–16128.
[7] T.P. Sakmar, S.T. Menon, E.P. Marin, E.S. Awad, Rhodopsin: insights from recent structural studies, Annu. Rev. Biophys. Biomol. Struct. 31 (2002) 443–484.
[8] W.L. Hubbell, C. Altenbach, C.M. Hubbell, H.G. Khorana, Rhodopsin structure, dynamics, and activation: a perspective from crystallography, site-directed spin labeling, sulfhydryl reactivity, and disulfide cross-linking, Adv. Protein Chem. 63 (2003) 243–290.
[9] J. Wess, S.-J. Han, S.-K. Kim, K.A. Jacobson, J.H. Li, Conformational changes involved in G-protein-coupled-receptor activation, Trends Pharmacol. Sci. 29 (2008) 616–625.
[10] C. Saunders, L.E. Limbird, Localization and trafficking of alpha2-adrenergic receptor subtypes in cells and tissues, Pharmacol. Ther. 84 (1999) 193–205.
[11] J.W. Kable, L.C. Murrin, D.B. Bylund, In vivo gene modification elucidates subtype-specific functions of alpha(2)-adrenergic receptors, J. Pharmacol. Exp. Ther. 293 (2000) 1–7.
[12] M. Brede, G. Nagy, M. Philipp, J.B. Sorensen, M.J. Lohse, L. Hein, Differential control of adrenal and sympathetic catecholamine release by alpha 2-adrenoceptor subtypes, Mol. Endocrinol. 17 (2003) 1640–1646.
[13] S. Uhlén, J.E. Wikberg, Delineation of rat kidney a_{2A}- and a_{2B}-adrenoceptors with [^{3}H]RX821002 radioligand binding: computer modelling reveals that guanfacine is an a_{2A}-selective compound, Eur. J. Pharmacol. 202 (1991) 235–243.
[14] H.D. Intengan, D.D. Smyth, Alpha-2a/d adrenoceptor subtype stimulation by guanfacine increases osmolar clearance, J. Pharmacol. Exp. Ther. 281 (1997) 48–52.
[15] P.A. Crassous, C. Cardinaletti, A. Carrieri, B. Bruni, M. Di Vaira, F. Gentili, F. Ghelfi, M. Giannella, H. Paris, A. Piergentili, W. Quaglia, S. Schaak, C. Vesprini, M. Pigini, α2-Adrenoreceptor profile modulation. 3.1 (R)-(+)-m-Nitrobiphenyline, a new efficient α2C-subtype selective agonist, J. Med. Chem. 50 (2007) 3964–3968.
[16] P. Young, J. Berge, H. Chapman, M.A. Cawthorne, Novel a_2-adrenoceptor antagonists show selectivity for a_{2A}- and a_{2B}-adrenoceptor subtypes, Eur. J. Pharmacol. 168 (1989) 381–386.

[17] J.P. Kiss, G. Zsilla, A. Mike, T. Zelles, E. Toth, A. Lajtha, E.S. Vizi, Subtype-specificity of the presynaptic alpha 2-adrenoceptors modulating hippocampal norepinephrine release in rat, Brain Res. 674 (1995) 238–244.
[18] J. Sallinen, I. Höglund, M. Engström, J. Lehtimäki, R. Virtanen, J. Sirviö, S. Wurster, J.M. Savola, A. Haapalinna, Pharmacological characterization and CNS effects of a novel highly selective alpha2C-adrenoceptor antagonist JP-1302, Br. J. Pharmacol. 150 (2007) 391–402.
[19] M.D. Tricklebank, JP-1302: a new tool to shed light on the roles of alpha2C-adrenoceptors in brain, Br. J. Pharmacol. 150 (2007) 381–382.
[20] L. Ostopovici-Halip, A. Borota, A. Gruia, M. Mracec, R. Rad-Curpan, M. Mracec, 3D homology model of the α2b-adrenergic receptor subtype, Rev. Roum. Chim. 55 (2010) 343–348.
[21] L. Ostopovici-Halip, A. Borota, M. Mracec, R. Rad-Curpan, A. Gruia, M. Mracec, 3D Homology model of the α2a-adrenergic receptor subtype, Rev. Roum. Chim. 54 (2009) 157–161.
[22] T. Okada, M. Sugihara, A.N. Bondar, M. Elstner, P. Entel, V. Buss, The retinal conformation and its environment in rhodopsin in light of a new 22 A crystal structure, J. Mol. Biol. 342 (2004) 571–583.
[23] K. Palczewski, T. Kumasaka, T. Hori, C.A. Behnke, H. Motoshima, B.A. Fox, I. Le Trong, D.C. Teller, T. Okada, R.E. Stenkamp, M. Yamamoto, M. Miyano, Crystal structure of rhodopsin: a G protein-coupled receptor, Science 289 (2000) 739–745.
[24] V. Cherezov, D.M. Rosenbaum, M.A. Hanson, S.G. Rasmussen, F.S. Thian, T.S. Kobilka, H.J. Choi, P. Kuhn, W.I. Weis, B.K. Kobilka, R.C. Stevens, High-resolution crystal structure of an engineered human beta2-adrenergic G protein-coupled receptor, Science 318 (2007) 1258–1265.
[25] A. Warne, M.J. Serrano-Vega, J.G. Baker, R. Moukhametzianov, P.C. Edwards, R. Henderson, A.G.W. Leslie, C.G. Tate, G.F.X. Schertler, Structure of the beta1-adrenergic G protein-coupled receptor, Nature 454 (2008) 486–491.
[26] M. Murakami, T. Kouyama, Crystal structure of squid rhodopsin, Nature 453 (2008) 363–367.
[27] V.P. Jaakola, M.T. Griffith, M.A. Hanson, V. Cherezov, E.Y. Chien, J.R. Lane, A.P. Ijzerman, R.C. Stevens, The 26 angstrom crystal structure of a human A2A adenosine receptor bound to an antagonist, Science 322 (2008) 1211–1217.
[28] F.F. Sherbiny, A.C. Schiedel, A. Maass, C.E. Muller, Homology modelling of the human adenosine A2B receptor based on X-ray structures of bovine rhodopsin, the beta2-adrenergic receptor and the human adenosine A2A receptor, J. Comput. Aided Mol. Des. 23 (2009) 807–828.
[29] C. Notredame, D.G. Higgins, J. Heringa, T-Coffee: a novel method for fast and accurate multiple sequence alignment, J. Mol. Biol. 302 (2000) 205–217.
[30] O. Poirot, E. O'Toole, C. Notredame, Tcoffee: a web server for computing, evaluating and combining multiple sequence alignments, Nucleic Acids Res. 31 (2003) 3503–3506.
[31] G.A. Kaminski, R.A. Friesner, J. Tirado-Rives, W.J.J. Jorgensen, Evaluation and reparametrization of the OPLS-AA force field for proteins via comparison with accurate quantum chemical calculations on peptides, J. Phys. Chem. B 105 (2001) 6474–6487.
[32] Protein Preparation Wizard; Schrodinger LLC, New York, NY 2007.
[33] J. Ballesteros, H. Weinstein, Integrated methods for the construction of the three-dimensional models and computational probing of structure–function relations in G-protein coupled receptors, Methods Neurosci. 25 (1995) 366–428.
[34] C.D. Wang, M.A. Buck, C.M. Fraser, Site-directed mutagenesis of alpha 2A-adrenergic receptors: identification of amino acids involved in ligand binding and receptor activation by agonists, Mol. Pharmacol. 40 (1991) 168–179.
[35] SiteMap version 2.1; Scrodinger LLC, New York, NY 2007.
[36] D.M. Rosenbaum, S.G.F. Rasmussen, B.K. Kobilka, The structure and function of G-protein-coupled receptors, Nature 459 (2009) 356–363.
[37] Glide 4.5; Schrodinger LLC, New York, NY 2008.
[38] Prime 1.6; Schrodinger LLC, New York, NY 2008.
[39] B. Balogh, A. Szilagyi, K. Gyires, D.B. Bylund, P. Matyus, Molecular modelling of subtypes (a2A, a2B and a2C) of a2-adrenoceptors: a comparative study, Neurochem. Int. 55 (2009) 355–436.
[40] J.M. Baldwin, G.F.X. Schertler, V.M. Unger, An alpha-carbon template for the transmembrane helices in the rhodopsin family of G-protein-coupled receptors, J. Mol. Biol. 272 (1997) 144–164.
[41] M. Olah, M. Mracec, L. Ostopovici, R. Rad, A. Bora, N. Hadaruga, I. Olah, M. Banda, Z. Simon, M. Mracec, T.I. Oprea, WOMBAT: world of molecular bioactivity, in: T.I. Oprea (Ed.), Chemoinformatics in Drug Discovery, Wiley-VCH, New York, 2004, pp. 223–239.
[42] M. Olah, R. Rad, L. Ostopovici, A. Bora, N. Hadaruga, R. Moldovan, A. Fulias, M. Mracec, T.I. Oprea, WOMBAT and WOMBAT-PK: bioactivity databases for lead and drug discovery, in: S.L. Schreiber, T.M. Kapoor, G. Wess (Eds.), Chemical Biology: From Small Molecules to Systems Biology and Drug Design, Wiley-VCH, New York, 2007, pp. 760–786.
[43] N. Huang, B.K. Shoichet, J.J. Irwin, Benchmarking sets for molecular docking, J. Med. Chem. 49 (2006) 6789–6801.
[44] DUD Release 2, http://dud.docking.org/r2/.
[45] V.M. Unger, P.A. Hargrave, J.M. Baldwin, G.F.X. Schertler, Arrangement of rhodopsin transmembrane alpha-helices, Nature 389 (1997) 203–206.
[46] D.B. Bylund, R.A. Bond, D.C. Eikenburg, J.P. Hieble, R. Hills, K.P. Minneman, S. Parra, Adrenoceptors: α2A-adrenoceptor IUPHAR database (IUPHAR-DB), http://wwwiuphar-dborg/GPCR/ReceptorDisplayForward?receptorID=2181 (accessed 09.09.09).
[47] S. Uhlen, A.C. Porter, R.R. Neubig, The novel alpha-2 adrenergic radioligand [3H]-MK912 is alpha-2C selective among human alpha-2A, alpha-2B and alpha-2C adrenoceptors, J. Pharmacol. Exp. Ther. 271 (1994) 1558–1565.
[48] A.D. Michel, D.N. Loury, R.L. Whiting, Assessment of imiloxan as a selective a2B-adrenoceptor antagonist, Br. J. Pharmacol. 99 (1990) 560–564.
[49] E.W. Willems, L.V. Valdivia, P.R. Saxena, C.M. Villalón, Pharmacological profile of the mechanisms involved in the external carotid vascular effects of the antimigraine agent isometheptene in anaesthetised dogs, Naunyn Schmiedebergs Arch. Pharmacol. 364 (2001) 27–32.
[50] S.C. Sinha, T.M. Heidelbaugh, S.S. Bhat, K. Chow, Substituted phenylmethyl imidazole compounds as subtype selective modulators of alpha-2B and/or alpha-2C adrenergic receptors (2009) WO 2009091735.
[51] T.M. Heidelbaugh, K. Chow, S.C. Sinha, P.X. Nguyen, W.K. Fang, L. Li, J.A. Takeuchi, S.S. Bhat, Preparation of oxazolidine and thiazolidine selective subtype alpha 2 adrenergic agents and methods for use thereof in therapy (2009) WO2009091759.
[52] B. Boeckmann, A. Bairoch, R. Apweiler, M.C. Blatter, A. Estreicher, E. Gasteiger, M.J. Martin, K. Michoud, C. O'Donovan, I. Phan, S. Pilbout, M. Schneider, The SWISS-PROT protein knowledgebase and its supplement TrEMBL, Nucleic Acids Res. 31 (2003) 365–370.
[53] E. Boutet, D. Lieberherr, M. Tognolli, M. Schneider, A. Bairoch, UniProtKB/Swiss-Prot, Methods Mol. Biol. 406 (2007) 89–112.
[54] A. Sali, T.L. Blundell, Comparative protein modelling by satisfaction of spatial restraints, J. Mol. Biol. 234 (1993) 779–815.
[55] N. Eswar, M.A. Marti-Renom, B. Webb, M.S. Madhusudhan, D. Eramian, M. Shen, U. Pieper, A. Sali, Comparative protein structure modeling with MODELLER, Curr. Protoc. Bioinform. 15 (2007) 561–5630.
[56] A. Fiser, R.K. Do, A. Sali, Modeling of loops in protein structures, Protein Sci. 9 (2000) 1753–1773.
[57] A. Fiser, A. Sali, ModLoop: automated modeling of loops in protein structures, Bioinformatics 19 (2003) 2500–2501.
[58] LigPrep version 21; Schrodinger, LLC, New York, NY 2007.
[59] Impact 4.5; Schrodinger, LLC, New York, NY 2007.
[60] InstantJChem 5.3.1, 2010, ChemAxon (http://www.chemaxon.com).